

Buckling and free flexural vibration of an asymmetric sandwich beam with a functionally graded core

K. MAGNUCKI¹⁾, E. MAGNUCKA-BLANDZI²⁾, K. SOWIŃSKI³⁾

¹⁾ *Łukasiewicz Research Network, Poznan Institute of Technology,
6 Ewarysta Estkowskiego St., 61-755 Poznan, Poland*

²⁾ *Institute of Mathematics, Poznan University of Technology,
Piotrowo 3A, 60-965 Poznan, Poland,
e-mail: ewa.magnucka-blandzi@put.poznan.pl (corresponding author)*

³⁾ *Institute of Applied Mechanics, Poznan University of Technology,
Piotrowo 3A, 60-965 Poznan, Poland*

THIS PAPER IS DEVOTED TO AN ASYMMETRICAL SANDWICH BEAM with a functionally graded core with three different variants of boundary conditions. An analytical model of this beam, considering individual nonlinear shear deformation theory, is developed. Based on Hamilton's principle, two differential equations of motion for this beam are obtained. These equations are solved analytically, and as a consequence, the critical forces and basic natural frequencies for each beam support variant are determined. Detailed calculations are carried out for selected exemplary beam structures, and their results are compared with numerical FEM analysis.

Key words: shear deformation theory, buckling, free vibration, sandwich structures.



Copyright © 2024 The Authors.

Published by IPPT PAN. This is an open access article under the Creative Commons Attribution License CC BY 4.0 (<https://creativecommons.org/licenses/by/4.0/>).

1. Introduction

COMPOSITE STRUCTURES, WHOSE DEVELOPMENT AND APPLICATION began in the last century, are currently the subject of intensive research. This is due to their superior performance-to-mass ratio compared to conventional materials. These structures can be tailored to meet very different requirements depending on their application by introducing spatially varying mechanical properties or selecting a specific number of layers and their characteristics. Such a design process can be especially beneficial in highly demanding industries, where the mechanical performance of structures is of utmost importance.

MAHI *et al.* [1] proposed a novel hyperbolic shear deformation theory considering five degrees of freedom that is applicable to the bending and free vibration analysis of isotropic, functionally graded sandwich and laminated composite plates. The theory implies parabolic transverse shear deformation across the thickness direction. NGUYEN *et al.* [2] introduced a new higher-order shear defor-

mation theory that allows solving the problems of buckling and free vibration of both isotropic and functionally graded sandwich beams. This approach was based on the hyperbolic distribution of transverse shear stress. CHEN *et al.* [3] investigated the free and forced vibration characteristics of functionally graded porous beams with nonuniform porosity distribution. This property was assumed to impact the elastic moduli and the mass density. The authors considered both symmetric and asymmetric porosity distributions.

FILIPPI and CARRERA [4] developed one-dimensional layer-wise theories based on higher-order zig-zag theory. The aim of their study was to formulate an approach with reduced computational cost while maintaining a satisfactory accuracy level. GONCALVES *et al.* [5] proposed a framework for linear buckling and free vibration analyses using a microstructure-dependent Timoshenko beam model. The problem was solved using a numerical finite element method approach by formulating an accurate, yet approximate, stiffness matrix. KITIPORNCHAI *et al.* [6] devoted their work to the problem of free vibration and elastic buckling of nanocomposite-layered porous beams reinforced with graphene platelets. The solution was achieved by referring to the Timoshenko beam theory and the Ritz method. MAGNUCKA-BLANDZI *et al.* [7] focused on the vibrations and stability of an untypical orthotropic layered beam, whose faces consisted of three layers. The modelling of the problem was based on Hamilton's principle, which allowed the derivation of the equations of motion.

MOHAMMADIMEHR and SHAHEDI [8] investigated higher-order buckling and free vibration analyses of sandwich beams characterised by aluminium alloy or polyvinyl chloride-form core and carbon nanotube-reinforced faces. The generalised differential quadrature method was used, while the core was studied using higher-order sandwich panel theory and the faces were considered within the framework of modified couple stress theory. ŻUR [9] presented research on analytical and numerical analyses of free axisymmetric and non-axisymmetric vibrations of functionally graded annular plates regarding classical plate theory. The author used quasi-Green's functions to solve the problem studied with different boundary conditions. ŻUR [10] also aimed to solve the problem of free vibrations of functionally graded circular plates elastically supported on a concentric ring using classical plate theory.

MAGNUCKI *et al.* [11] referred to the Zhuravsky shear stress formula to develop a shear deformation theory for simply supported beams with bi-symmetrical cross sections under generalised load. XIE *et al.* [12] devoted their work to the analysis of nonlinear free vibration of functionally graded beams using various theories of shear deformation. The von Kármán geometric nonlinearity was included in the investigated problem, while the Ritz method and Lagrange equation were considered to achieve the solution. LEI *et al.* [13] focused on the dynamic behaviour of single and multi-span functionally graded porous beams with elastic

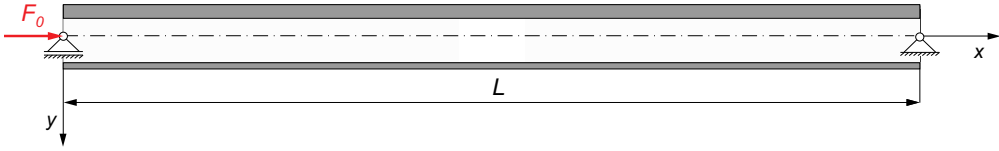
boundary conditions. Hamilton's principle within the framework of Timoshenko beam theory was applied and solved based on the singular convolution element method.

LE *et al.* [14] formulated a third-order shear deformation beam element for free vibration and buckling analysis of bidirectional functionally graded sandwich beams. It is derived using hierarchical functions to enrich the Lagrange and Hermite interpolations of a conventional beam element. MAGNUCKA-BLANDZI *et al.* [15] studied the bending and buckling problems of a simply supported circular plate. The assumed generalised form of symmetrically varying mechanical properties enables the study of both single-layer and three-layer structures within a consistent mathematical formulation that includes the shear effect. HUNG *et al.* [16] investigated thermally induced free vibrations of sandwich beams with a functionally graded porous core and isotropic faces. The authors referred to third-order and quasi-3D beam theories within the framework of a mesh-free approach based on the point interpolation technique.

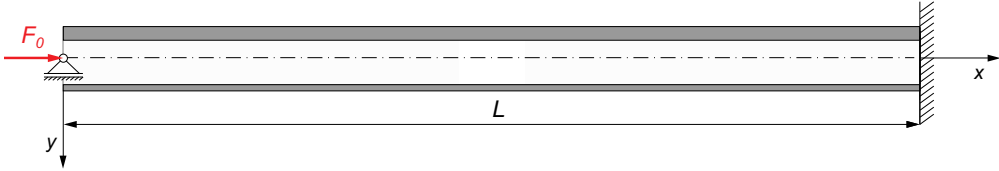
MAGNUCKI *et al.* [17] analysed the buckling and free vibration problems of simply supported sandwich beams. Three models of the structures were taken into consideration, while two nonlinear individual shear theories of deformation were proposed. MAGNUCKI *et al.* [18] presented bending problem of generalised circular sandwich plate with consideration of the individual nonlinear shear deformation theory. WANG *et al.* [19] combined the absolute nodal coordinate formulation with zig-zag theory to achieve an efficient numerical approach to solve the problems of static deformation and free vibrations of sandwich beams. GOLIWAŚ *et al.* [20] devoted their work to elastic buckling of the sandwich beam with three different supports. Using the principle of stationary total potential energy, two nonlinear differential equations of equilibrium were obtained and analytically solved, including the exemplary equilibrium paths. MAGNUCKI and MAGNUCKA-BLANDZI [21] studied the static behaviour of a sandwich beam with an asymmetric structure and a functionally graded and homogeneous core under a uniformly distributed load. The individual nonlinear shear deformation function was analytically developed, taking into account the classical shear stress formula to calculate displacements, strains, and stresses.

Following the provided references, numerous aspects of composite structures require further studies, especially in terms of unified formulations allowing for the evaluation of their mechanical behaviour. Many researchers provide approximate but accurate solutions achieved within the framework of numerical methods. On the contrary, an analytical approach that provides a closed-form solution can be considered more useful because the relationship between the varying mechanical properties of composites and their performance is evident and does not require parametric studies.

(a) simply supported – **B-1**



(b) simply supported at one end and clamped at the other – **B-2**



(c) clamped ends – **B-3**

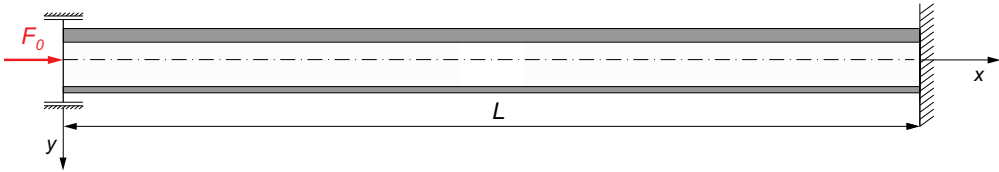


FIG. 1. Schemes of the asymmetric sandwich beam with three different types of supports.

The subject of the paper is an asymmetric sandwich beam with a functionally graded core of length L , with three different types of supports under the action of an axial compressive force F_o along the neutral axis (Fig. 1).

The cross section of this beam is a rectangle with width b and total depth h . Furthermore, the thicknesses of successive layers are as follows: h_{f1} – the upper face, h_c – the core, h_{f2} – the lower face (Fig. 2). The studied beam constitutes a combination of sandwich structure and functionally graded structure. The faces are considered to be homogeneous, whereas the mechanical properties of the core

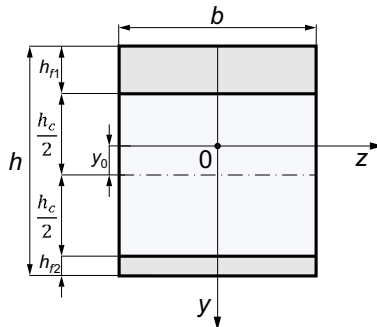


FIG. 2. Scheme of the cross section of this beam with an asymmetric structure.

vary in the thickness direction. It is assumed that the mechanical properties are continuous; thus, the Young's modulus of the core is consistent with that of the faces at their junction.

The main purpose of this work is to analytically study the buckling and free flexural vibration problems of the asymmetric sandwich beam with functionally graded core. This work is a continuation of previous research on the bending behavior of the asymmetric sandwich beam presented in [21].

2. Analytical model of the asymmetric sandwich beam

The variation of Young's modulus in successive layers of this beam is as follows:

- the upper face ($-\chi_{f1} - \chi_c/2 + \eta_0 \leq \eta \leq -\chi_c/2 + \eta_0$)

$$(2.1) \quad E_f(\eta) = E_f = \text{const},$$

- the porous core ($-\chi_c/2 + \eta_0 \leq \eta \leq \chi_c/2 + \eta_0$)

$$(2.2) \quad E_c(\eta) = E_f \cdot f_e^{(c)}(\eta),$$

- the lower face ($\chi_c/2 + \eta_0 \leq \eta \leq \chi_{f2} + \chi_c/2 + \eta_0$)

$$(2.3) \quad E_f(\eta) = E_f = \text{const},$$

where the dimensionless function of the core:

$$(2.4) \quad f_e^{(c)}(\eta) = e_c + (1 - e_c) \sin^n \left[\frac{\pi}{\chi_c} (\eta - \eta_0) \right],$$

where the dimensionless coordinate $\eta = y/h$, the neutral axis position $\eta_0 = y_0/h$, the coefficient of the core e_c , the dimensionless thicknesses of the layers are $\chi_{f1} = h_{f1}/h$ (upper face), $\chi_c = h_c/h$ (core), $\chi_{f2} = h_{f2}/h$ (lower face), and a natural number exponent is n .

The graph of Young's modulus variability in the depth direction of this beam is presented in Fig. 3. The character of this variability is motivated by the applicability of three-layered structures due to their superior strength-to-mass ratio compared to homogeneous structures. The proposed distribution constitutes a generalised three-layered, structure which also enables one to describe and solve problems of isotropic beams. Such variability can be achieved by introducing a porosity, using a variable mixture of different materials, or by designing a specific cross-sectional geometry to be produced using additive manufacturing techniques. Unlike typical three-layered sandwich structures, the introduced model maintains continuity of stiffness due to the considered functionally graded core.

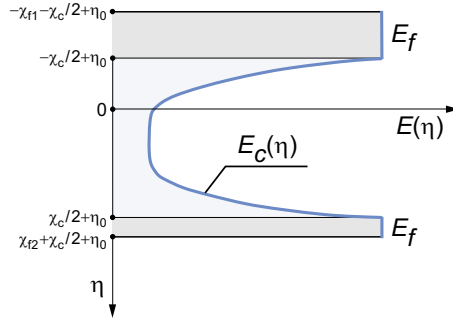


FIG. 3. Graph of the Young’s modulus variability in the depth direction of the beam.

The dimensionless coordinate η_0 of the neutral axis position is calculated based on the zeroing condition of the first moment of the beam cross section, with consideration of Young’s modulus, in the following form:

$$(2.5) \quad \bar{S}_z^{(uf)} + \bar{S}_z^{(c)} + \bar{S}_z^{(lf)} = 0,$$

where

$$\begin{aligned} \bar{S}_z^{(uf)} &= -\frac{1}{2}(\chi_{f1} + \chi_c - 2\eta_0)\chi_{f1}, \\ \bar{S}_z^{(lf)} &= \frac{1}{2}(\chi_{f2} + \chi_c + 2\eta_0)\chi_{f2}, \\ \bar{S}_z^{(c)} &= e_c\chi_c\eta_0 + (1 - e_c) \int_{-\chi_c/2+\eta_0}^{\chi_c/2+\eta_0} \eta \sin^n \left[\frac{\pi}{\chi_c}(\eta - \eta_0) \right] d\eta. \end{aligned}$$

The deformation scheme of a plane cross section after bending of this sandwich beam is presented in Fig. 4.

Taking into account Fig. 4, the longitudinal displacements, and consequently, the strains and stresses in successive layers are as follows:

- the upper face $(-\chi_{f1} - \chi_c/2 + \eta_0 \leq \eta \leq -\chi_c/2 + \eta_0)$:

$$(2.6) \quad u^{(uf)}(x, \eta, t) = -h \left[\eta \frac{\partial v}{\partial x} - f_d^{(uf)}(\eta) \psi(x, t) \right],$$

$$(2.7) \quad \varepsilon_x^{(uf)}(x, \eta, t) = -h \left[\eta \frac{\partial^2 v}{\partial x^2} - f_d^{(uf)}(\eta) \frac{\partial \psi}{\partial x} \right], \quad \gamma_{xy}^{(uf)}(x, \eta, t) = \frac{df_d^{(uf)}}{d\eta} \psi(x, t),$$

$$(2.8) \quad \sigma_x^{(uf)}(x, \eta, t) = E_f \varepsilon_x^{(uf)}(x, \eta, t), \quad \tau_{xy}^{(uf)}(x, \eta, t) = \frac{E_f}{2(1 + \nu)} \gamma_{xy}^{(uf)}(x, \eta, t);$$

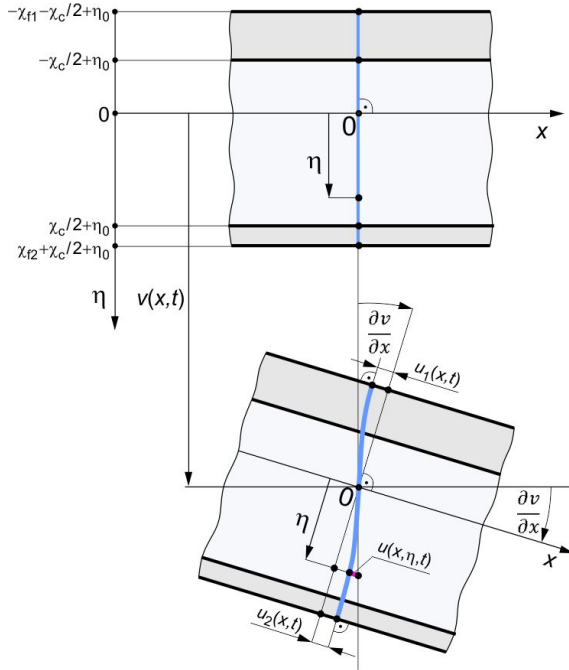


FIG. 4. Scheme of the deformation of a planar cross section of the sandwich beam under study.

- the core ($-\chi_c/2 + \eta_0 \leq \eta \leq \chi_c/2 + \eta_0$):

$$(2.9) \quad u^{(c)}(x, \eta, t) = -h \left[\eta \frac{\partial v}{\partial x} - f_d^{(c)}(\eta) \psi(x, t) \right],$$

$$(2.10) \quad \varepsilon_x^{(c)}(x, \eta, t) = -h \left[\eta \frac{\partial^2 v}{\partial x^2} - f_d^{(c)}(\eta) \frac{\partial \psi}{\partial x} \right], \quad \gamma_{xy}^{(c)}(x, \eta, t) = \frac{df_d^{(c)}}{d\eta} \psi(x, t),$$

$$(2.11) \quad \begin{aligned} \sigma_x^{(c)}(x, \eta, t) &= E_f \varepsilon_x^{(c)}(x, \eta, t) \cdot f_e^{(c)}(\eta), \\ \tau_{xy}^{(c)}(x, \eta, t) &= \frac{E_f}{2(1 + \nu)} \gamma_{xy}^{(c)}(x, \eta, t) \cdot f_e^{(c)}(\eta); \end{aligned}$$

- the lower face ($\chi_c/2 + \eta_0 \leq \eta \leq \chi_{f2} + \chi_c/2 + \eta_0$):

$$(2.12) \quad u^{(lf)}(x, \eta) = -h \left[\eta \frac{dv}{dx} - f_d^{(lf)}(\eta) \psi(x) \right],$$

$$(2.13) \quad \varepsilon_x^{(lf)}(x, \eta, t) = -h \left[\eta \frac{\partial^2 v}{\partial x^2} - f_d^{(lf)}(\eta) \frac{\partial \psi}{\partial x} \right], \quad \gamma_{xy}^{(lf)}(x, \eta, t) = \frac{df_d^{(lf)}}{d\eta} \psi(x, t),$$

$$(2.14) \quad \sigma_x^{(lf)}(x, \eta, t) = E_f \varepsilon_x^{(lf)}(x, \eta, t), \quad \tau_{xy}^{(lf)}(x, \eta, t) = \frac{E_f}{2(1 + \nu)} \gamma_{xy}^{(lf)}(x, \eta, t),$$

where $v(x,t)$ – the deflection, $\psi(x,t)$ – the dimensionless longitudinal displacement function, ν – Poisson’s ratio, $f_d^{(uf)}(\eta)$, $f_d^{(c)}(\eta)$, $f_d^{(lf)}(\eta)$ – the dimensionless deformation functions.

The unknown dimensionless deformation functions $f_d^{(uf)}(\eta)$, $f_d^{(c)}(\eta)$, $f_d^{(lf)}(\eta)$ are determined with consideration of the classical shear stress formula, similarly to that in [20]. Thus, these functions for successive layers are as follows:

- the upper face ($-\chi_{f1} - \chi_c/2 + \eta_0 \leq \eta \leq -\chi_c/2 + \eta_0$):

$$(2.15) \quad f_d^{(uf)}(\eta) = C_{f1} + \frac{1}{2} \left[\left(\chi_{f1} + \frac{1}{2} \chi_c - \eta_0 \right)^2 - \frac{1}{3} \eta^2 \right] \eta;$$

- the core ($-\chi_c/2 + \eta_0 \leq \eta \leq \chi_c/2 + \eta_0$):

$$(2.16) \quad f_d^{(c)}(\eta) = \int \frac{\bar{Q}_z^{(c)}(\eta)}{f_e^{(c)}(\eta)} d\eta;$$

- the lower face ($\chi_c/2 + \eta_0 \leq \eta \leq \chi_{f2} + \chi_c/2 + \eta_0$):

$$(2.17) \quad f_d^{(lf)}(\eta) = C_{f2} + \frac{1}{2} \left[\left(\chi_{f2} + \frac{1}{2} \chi_c - \eta_0 \right)^2 - \frac{1}{3} \eta^2 \right] \eta,$$

where

$$\bar{Q}_z^{(c)}(\eta) = \frac{1}{2} \left\{ (\chi_{f1} + \chi_c - 2\eta_0) \chi_{f1} + \left[\left(\frac{1}{2} \chi_c - \eta_0 \right)^2 - \eta^2 \right] e_c - 2(1 - e_c) J_{c1}(\eta) \right\},$$

$$C_{f1} = \frac{1}{2} \left[\left(\chi_{f1} + \frac{1}{2} \chi_c - \eta_0 \right)^2 - \frac{1}{3} \left(\frac{1}{2} \chi_c - \eta_0 \right)^2 \right] \left(\frac{1}{2} \chi_c - \eta_0 \right) - \int_{-\chi_c/2 + \eta_0}^0 \frac{\bar{Q}_z^{(c)}(\eta)}{f_e^{(c)}(\eta)} d\eta,$$

$$C_{f2} = -\frac{1}{2} \left[\left(\chi_{f2} + \frac{1}{2} \chi_c + \eta_0 \right)^2 - \frac{1}{3} \left(\frac{1}{2} \chi_c + \eta_0 \right)^2 \right] \left(\frac{1}{2} \chi_c + \eta_0 \right) + \int_0^{\chi_c/2 + \eta_0} \frac{\bar{Q}_z^{(c)}(\eta)}{f_e^{(c)}(\eta)} d\eta,$$

$$J_{c1}(\eta) = \int_{-\chi_c/2 + \eta_0}^{\eta} \eta_1 \sin^n \left[\frac{\pi}{\chi_c} (\eta_1 - \eta_0) \right] d\eta_1.$$

3. Analytical study of buckling and free flexural vibration problems

The kinetic energy is given by:

$$(3.1) \quad U_k = \frac{1}{2} \rho_b b h \int_0^L \left(\frac{\partial v}{\partial t} \right)^2 dx,$$

where

$$\rho_b = \left\{ \chi_{f1} + \chi_{f2} + \sqrt{e_c} \chi_c + (1 - \sqrt{e_c}) \int_{-\chi_c/2+\eta_0}^{\chi_c/2+\eta_0} \sin^n \left[\frac{\pi}{\chi_c} (\eta - \eta_0) \right] d\eta \right\} \rho_f$$

is the mass density of the beam, ρ_f – the mass density of the faces, and t – time.

The elastic strain energy is given by:

$$(3.2) \quad U_{es} = \frac{1}{2}bh \int_0^L [\Phi_{\varepsilon,\gamma}^{(uf)}(x, t) + \Phi_{\varepsilon,\gamma}^{(c)}(x, t) + \Phi_{\varepsilon,\gamma}^{(lf)}(x, t)] dx,$$

where:

$$\begin{aligned} \Phi_{\varepsilon,\gamma}^{(uf)}(x) &= \int_{-\chi_{f1}-\chi_c/2+\eta_0}^{-\chi_c/2+\eta_0} [\sigma_x^{(uf)}(x, \eta, t) \cdot \varepsilon_x^{(uf)}(x, \eta, t) + \tau_{xy}^{(uf)}(x, \eta, t) \cdot \gamma_{xy}^{(uf)}(x, \eta, t)] d\eta, \\ \Phi_{\varepsilon,\gamma}^{(c)}(x, t) &= \int_{-\chi_c/2+\eta_0}^{\chi_c/2+\eta_0} [\sigma_x^{(c)}(x, \eta, t) \cdot \varepsilon_x^{(c)}(x, \eta, t) + \tau_{xy}^{(c)}(x, \eta, t) \cdot \gamma_{xy}^{(c)}(x, \eta, t)] d\eta, \\ \Phi_{\varepsilon,\gamma}^{(lf)}(x, t) &= \int_{\chi_c/2+\eta_0}^{\chi_{f2}+\chi_c/2+\eta_0} [\sigma_x^{(lf)}(x, \eta, t) \cdot \varepsilon_x^{(lf)}(x, \eta, t) + \tau_{xy}^{(lf)}(x, \eta, t) \cdot \gamma_{xy}^{(lf)}(x, \eta, t)] d\eta. \end{aligned}$$

The work of the load is as follows:

$$(3.3) \quad W = \frac{1}{2}F_o \int_0^L \left(\frac{\partial v}{\partial x} \right)^2 dx.$$

Based on Hamilton’s principle:

$$(3.4) \quad \delta \int_{t_1}^{t_2} [U_k - (U_{es} - W)] dt = 0,$$

two differential equations of motion are obtained in the following form:

$$(3.5) \quad \rho_b bh \frac{\partial^2 v}{\partial t^2} + E_f bh^3 \left(C_{vv} \frac{\partial^4 v}{\partial x^4} - C_{v\psi} \frac{\partial^3 \psi}{\partial x^3} \right) + F_o \frac{\partial^2 v}{\partial x^2} = 0,$$

$$(3.6) \quad C_{v\psi} \frac{\partial^3 v}{\partial x^3} - C_{\psi\psi} \frac{\partial^2 \psi}{\partial x^2} + C_{\psi} \frac{\psi(x, t)}{h^2} = 0,$$

where dimensionless coefficients are as follows:

$$\begin{aligned}
 C_{vv} &= \int_{-\chi_{f1}-\chi_c/2+\eta_0}^{-\chi_c/2+\eta_0} \eta^2 d\eta + \int_{-\chi_c/2+\eta_0}^{\chi_c/2+\eta_0} \eta^2 f_e^{(c)}(\eta) d\eta + \int_{\chi_c/2+\eta_0}^{\chi_{f2}+\chi_c/2+\eta_0} \eta^2 d\eta, \\
 C_{v\psi} &= \int_{-\chi_{f1}-\chi_c/2+\eta_0}^{-\chi_c/2+\eta_0} f_d^{(uf)}(\eta) \eta d\eta + \int_{-\chi_c/2+\eta_0}^{\chi_c/2+\eta_0} f_d^{(c)}(\eta) \cdot f_e^{(c)}(\eta) \eta d\eta \\
 &+ \int_{\chi_c/2+\eta_0}^{\chi_{f2}+\chi_c/2+\eta_0} f_d^{(lf)}(\eta) \eta d\eta, \\
 C_{\psi\psi} &= \int_{-\chi_{f1}-\chi_c/2+\eta_0}^{-\chi_c/2+\eta_0} [f_d^{(uf)}(\eta)]^2 d\eta + \int_{-\chi_c/2+\eta_0}^{\chi_c/2+\eta_0} [f_d^{(c)}(\eta)]^2 f_e^{(c)}(\eta) d\eta \\
 &+ \int_{\chi_c/2+\eta_0}^{\chi_{f2}+\chi_c/2+\eta_0} [f_d^{(lf)}(\eta)]^2 d\eta, \\
 C_\psi &= \frac{1}{2(1+\nu)} \left\{ \int_{-\chi_{f1}-\chi_c/2+\eta_0}^{-\chi_c/2+\eta_0} \left(\frac{df_d^{(uf)}}{d\eta} \right)^2 d\eta + \int_{-\chi_c/2+\eta_0}^{\chi_c/2+\eta_0} \left(\frac{df_d^{(uf)}}{d\eta} \right)^2 f_e^{(c)}(\eta) d\eta \right. \\
 &\left. + \int_{\chi_c/2+\eta_0}^{\chi_{f2}+\chi_c/2+\eta_0} \left(\frac{df_d^{(lf)}}{d\eta} \right)^2 d\eta \right\}.
 \end{aligned}$$

3.1. The buckling problem

Taking into account the equations of motion (3.5) and (3.6), the system of two equations of equilibrium for a static buckling problem is as follows:

$$\begin{aligned}
 (3.7) \quad C_{vv} \frac{d^4 v}{dx^4} - C_{v\psi} \frac{d^3 \psi}{dx^3} + \frac{F_o}{E_f b h^3} \frac{d^2 v}{dx^2} &= 0, \\
 C_{v\psi} \frac{d^3 v}{dx^3} - C_{\psi\psi} \frac{d^2 \psi}{dx^2} + C_\psi \frac{\psi(x)}{h^2} &= 0.
 \end{aligned}$$

This system is approximately solved with two assumed functions: $v(x)$ – the deflection and $\psi(x)$ – the dimensionless longitudinal displacement. The buckling problem of the beam on three different types of supports, with consideration of the paper [19], is studied:

- Simply supported – **B-1** (Fig. 1a):

$$(3.8) \quad v(x) = v_a \sin\left(\pi \frac{x}{L}\right), \quad \psi(x) = \psi_a \cos\left(\pi \frac{x}{L}\right),$$

where v_a, ψ_a – parameters of the functions.

These functions satisfy the following boundary-supported conditions: $v(0) = v(L) = 0, d\psi/dx|_0 = d\psi/dx|_L = 0$. Substituting these functions (3.8) into Eqs. (3.7), after a simple transformation, one obtains the homogeneous algebraic equation system, from which the critical force is in the form:

$$(3.9) \quad F_{o,CR}^{(B-1)} = \bar{F}_{o,CR}^{(B-1)} \cdot E_f b h,$$

where the dimensionless critical force is:

$$(3.10) \quad \bar{F}_{o,CR}^{(B-1)} = (1 - C_{se}^{(B-1)}) \frac{\pi^2}{\lambda^2} C_{vv},$$

and the shear coefficient:

$$(3.11) \quad C_{se}^{(B-1)} = \frac{\pi^2 C_{v\psi}^2}{\pi^2 C_{\psi\psi} + \lambda^2 C_{\psi}} \cdot \frac{1}{C_{vv}},$$

where $\lambda = L/h$ – the relative length of the beam.

- Simply supported at one end and clamped at the other – **B-2** (Fig. 1b):

$$(3.12) \quad v(x) = v_a \left[\frac{x}{L} - \frac{\sin(kx/L)}{\sin k} \right], \quad \psi(x) = \psi_a \left[1 - k \frac{\cos(kx/L)}{\sin k} \right],$$

where the coefficient $k = \pi/0.6991557 \cong 4.493409 \Rightarrow k/\tan k = 1$.

Assuming this specific value of the parameter k , these functions satisfy the following boundary-supported conditions: $v(0) = v(L) = dv/dx|_L = 0, d\psi/dx|_0 = \psi(L) = 0$. Using the Galerkin method after substituting functions (3.12) into Eqs. (3.7), allows one to calculate the critical force:

$$(3.13) \quad F_{o,CR}^{(B-2)} = \bar{F}_{o,CR}^{(B-2)} \cdot E_f b h,$$

where the dimensionless critical force:

$$(3.14) \quad \bar{F}_{o,CR}^{(B-2)} = (1 - C_{se}^{(B-2)}) \frac{k^2}{\lambda^2} C_{vv},$$

and the shear coefficient:

$$(3.15) \quad C_{se}^{(B-2)} = \frac{k^2 C_{v\psi}^2}{k^2 C_{\psi\psi} + \lambda^2 C_{\psi}} \cdot \frac{1}{C_{vv}}.$$

- Clamped ends – **B-3** (Fig. 1c):

$$(3.16) \quad v(x) = \frac{1}{2}v_a \left[1 - \cos\left(2\pi \frac{x}{L}\right) \right], \quad \psi(x) = \psi_a \sin\left(2\pi \frac{x}{L}\right).$$

These functions satisfy the following boundary-supported conditions: $v(0) = v(L) = dv/dx|_0 = dv/dx|_L = 0$, $\psi(0) = \psi(L) = 0$. Inserting functions (3.16) into Eqs. (3.7) following some rearrangements leads to the expression for the critical force:

$$(3.17) \quad F_{o,CR}^{(B-3)} = \bar{F}_{o,CR}^{(B-3)} \cdot E_f b h,$$

where the dimensionless critical force:

$$(3.18) \quad \bar{F}_{o,CR}^{(B-3)} = (1 - C_{se}^{(B-3)}) \frac{4\pi^2}{\lambda^2} C_{vv},$$

and the shear coefficient:

$$(3.19) \quad C_{se}^{(B-3)} = \frac{4\pi^2 C_{v\psi}^2}{4\pi^2 C_{\psi\psi} + \lambda^2 C_{\psi}} \cdot \frac{1}{C_{vv}}.$$

3.2. The free flexural vibration problem

The two differential equations of motion (3.5) and (3.6) neglecting the axial force F_o are of the form:

$$(3.20) \quad \begin{aligned} \frac{\rho_b}{E_f h^2} \frac{\partial^2 v}{\partial t^2} + C_{vv} \frac{\partial^4 v}{\partial x^4} - C_{v\psi} \frac{\partial^3 \psi}{\partial x^3} &= 0, \\ C_{v\psi} \frac{\partial^3 v}{\partial x^3} - C_{\psi\psi} \frac{\partial^2 \psi}{\partial x^2} + C_{\psi} \frac{\psi(x, t)}{h^2} &= 0. \end{aligned}$$

This system is approximately solved, similarly to the buckling problem, with two assumed functions: $v(x, t)$ – the deflection and $\psi(x, t)$ – the dimensionless longitudinal displacement. The free flexural vibration problem of the beam on three different types of supports is studied:

- Simply supported – **B-1** (Fig. 1a):

$$(3.21) \quad v(x, t) = v_a(t) \sin\left(\pi \frac{x}{L}\right), \quad \psi(x, t) = \psi_a(t) \cos\left(\pi \frac{x}{L}\right),$$

where $v_a(t)$, $\psi_a(t)$ – the functions of time.

Substituting these functions (3.21) into Eqs. (3.20), after a simple transformation, one obtains the following differential equation:

$$(3.22) \quad \frac{\rho_b}{E_f} \frac{d^2 v_a}{dt^2} + \frac{\pi^4}{\lambda^2 L^2} (1 - C_{se}^{(B-1)}) C_{vv} v_a(t) = 0.$$

This equation (3.22) is approximately solved with the assumption of the function:

$$(3.23) \quad v_a(t) = v_a \sin(\omega t),$$

where v_a [mm] – the amplitude of the flexural vibration, and ω [rad/s] – the fundamental natural frequency. The fundamental natural frequency can be obtained by substituting the function (3.23) into Eq. (3.22), which results in:

$$(3.24) \quad f_z^{(B-1)} = \frac{\omega}{2\pi} = \frac{\pi \cdot 10^3}{2\lambda L} \sqrt{(1 - C_{se}^{(B-1)}) \frac{E_f}{\rho_b} C_{vv}} \text{ [Hz]},$$

where dimensions of quantities: E_f [MPa], ρ_b [kg/m³] and length L [m].

- Simply supported at one end and clamped at the other – **B-2** (Fig. 1b):

$$(3.25) \quad \begin{aligned} v(x, t) &= v_a(t) \left[\frac{x}{L} - \frac{\sin(kx/L)}{\sin k} \right], \\ \psi(x, t) &= \psi_a(t) \left[1 - k \frac{\cos(kx/L)}{\sin k} \right]. \end{aligned}$$

Using the expressions in Eqs. (3.20), applying them to the functions (3.25), and referring to the Galerkin method, enables derivation of the following differential equation:

$$(3.26) \quad \frac{\rho_b}{E_f} \frac{d^2 v_a}{dt^2} + \frac{3}{5} \frac{k^4}{\lambda^2 L^2} (1 - C_{se}^{(B-2)}) C_{vv} v_a(t) = 0.$$

This equation (3.26) is approximately solved with the assumption of the function from Eq. (3.23). The fundamental natural frequency is then as follows:

$$(3.27) \quad f_z^{(B-2)} = \frac{\omega}{2\pi} = \frac{k^2 \cdot 10^3}{2\pi \lambda L} \sqrt{\frac{3}{5} (1 - C_{se}^{(B-2)}) \frac{E_f}{\rho_b} C_{vv}} \text{ [Hz]}.$$

- Clamped ends – **B-3** (Fig. 1c):

$$(3.28) \quad v(x, t) = \frac{1}{2} v_a(t) \left[1 - \cos\left(2\pi \frac{x}{L}\right) \right], \quad \psi(x) = \psi_a(t) \sin\left(2\pi \frac{x}{L}\right).$$

Proceeding in the same way as for beam **B-1**, one obtains the fundamental natural frequency as:

$$(3.29) \quad f_z^{(B-3)} = \frac{\omega}{2\pi} = \frac{2\pi \cdot 10^3}{\lambda L} \sqrt{\frac{1}{3} (1 - C_{se}^{(B-3)}) \frac{E_f}{\rho_b} C_{vv}} \text{ [Hz]}.$$

4. Example detailed calculations

An exemplary analytical study is carried out for beams of a relative length $\lambda = 30$, Poisson's ratio $\nu = 0.3$, coefficient of the core $e_c = 1/30$, the exponent $n = 14$ with three selected sandwich structures (Table 1) and the following material parameters: $E_f = 72$ GPa, $\rho_f = 2710$ kg/m³.

TABLE 1. The values of dimensionless sizes of three beam structures: S-1, S-2, S-3.

Structure	S-1	S-2	S-3
χ_{f1}	8/40	7/40	6/40
χ_c	28/40	28/40	28/40
χ_{f2}	4/40	5/40	6/40
η_0	0.1075092	0.0537546	0

The results of example calculations: the values of the shear coefficient, critical force, and fundamental natural frequency for beams B-1, B-2, and B-3 are specified in Tables 2, 3, 4, respectively. Due to the ability to include the shear effect in the proposed analytical model, additional calculations are carried out considering the decrease in the relative length λ , as shown in Table 5. This could potentially indicate the limits of applicability of the proposed model when compared to the numerical study described further in the paper.

TABLE 2. The results of example calculations for beam **B-1** (Fig. 1a).

Structure	S-1	S-2	S-3
$C_{se}^{(B-1)}$	0.0357022	0.0372337	0.0377453
$10^3 \bar{F}_{o,CR}^{(B-1)}$ [-]	0.69880	0.72046	0.72766
$f_z^{(B-1)}$ [Hz]	76.717	77.897	78.285

TABLE 3. The results of example calculations for beam **B-2** (Fig. 1b).

Structure	S-1	S-2	S-3
$C_{se}^{(B-2)}$	0.0700697	0.0731603	0.0741940
$10^3 \bar{F}_{o,CR}^{(B-2)}$ [-]	1.37861	1.41887	1.43222
$f_z^{(B-2)}$ [Hz]	119.382	121.112	121.681

TABLE 4. The results of example calculations for beam **B-3** (Fig. 1c).

Structure	S-1	S-2	S-3
$C_{se}^{(B-3)}$	0.1273356	0.1332095	0.1351787
$10^3 \bar{F}_{o,CR}^{(B-3)}$ [-]	2.52957	2.59454	2.61592
$f_z^{(B-3)}$ [Hz]	168.542	170.692	171.394

TABLE 5. The results of example calculations for beam **B-1** (Fig. 1c) and **S-1** structure for various relative length λ .

λ [-]	15	20	25
$C_{se}^{(B-1)}$	0.1273356	0.0764587	0.0505109
$10^3 F_{\alpha,CR}^{(B-1)}$ [-]	2.52957	1.50584	0.99082
$f_z^{(B-1)}$ [Hz]	291.923	168.925	109.620

5. Numerical FEM study

To verify the results of the derived analytical model, the studied beams are investigated numerically using FEM analyses conducted in ANSYS 2023 R2 software. Both modal and buckling analyses are performed. Taking into account the non-dimensional form of the analytical calculations, the following exemplary values of geometric parameters are assumed in the numerical model: $b = h = 40$ mm and $L = 1200$ mm, thus $\lambda = 30$. The Young's modulus of the faces is set to $E_f = 72$ GPa, while the density $\rho_f = 2710$ kg/m³ which corresponds to aluminium alloys.

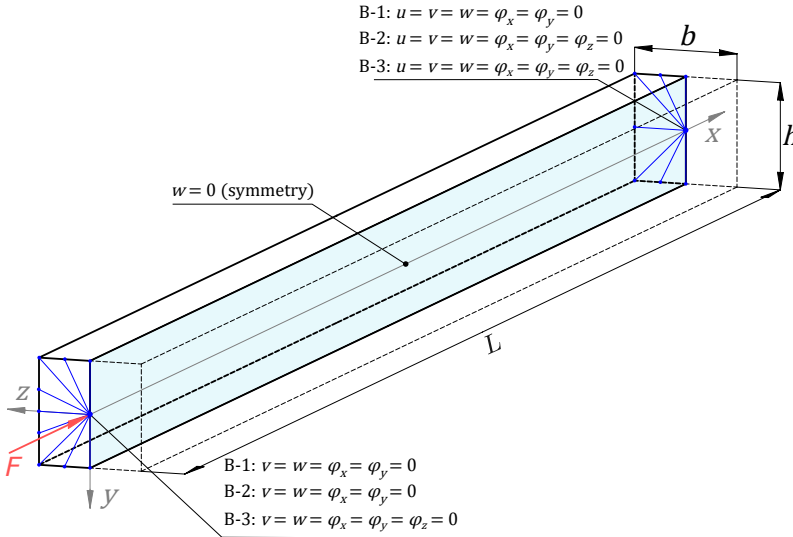


FIG. 5. Geometry and boundary conditions in the numerical model.

To simplify the numerical model, only half of the beam is studied due to the expected symmetry in the xy plane, as shown in Fig. 5. The boundary conditions reflect the structural behaviour of the beams investigated in the analytical study, as presented in Fig. 5. Following the analytical study, the beam core has non-homogeneous properties and follows exactly the Young's modulus distribution

given in Eqs. (2.2) and (2.4). The calculated values of this mechanical property are assigned to the centres of finite elements, while their sufficient number ensures an accurate and smooth distribution of Young's modulus.

The geometry of the beam is divided into uniform first-order hexahedral finite elements with 8 nodes and 24 degrees of freedom described as SOLID185 in the ANSYS software. The choice of first-order elements is motivated by the fact that the precision of Young's modulus distribution depends on the number of finite elements. When comparing models divided into first- and second-order elements with the same number of nodes, the latter provides a significantly smaller number of finite elements. To ensure satisfactory quality of the results, a mesh convergence study is conducted, focusing on the critical load and natural frequency as criteria. It is concluded that when a numerical model consists of 300, 90 and 10 elements along x , y , z directions (Fig. 5), upon further increase of the number of elements, leads to a marginal difference in results. Thus, such a model is used in the numerical study. It is important to note that the size of finite elements in the core towards y direction is half the size of the elements in the faces. This is because there is no necessity for a highly accurate mesh for isotropic material. The segment of the beam divided into finite elements is shown in Fig. 6, whereas an exemplary Young's modulus distribution is presented in Fig. 7.

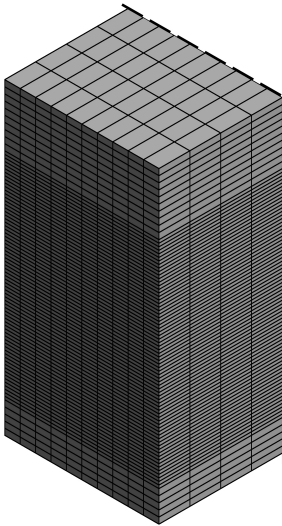


FIG. 6. Segment of the beam divided into finite elements.

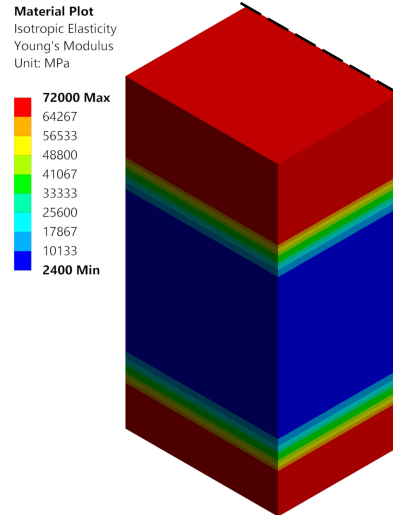


FIG. 7. Young's modulus distribution in the segment of the beam.

Exemplary results are shown in Figs. 8 and 9 for selected vibration and buckling analyses, respectively. The latter is obtained by applying a compressive force of 1 kN. Taking into account the load multiplier and the compressive force

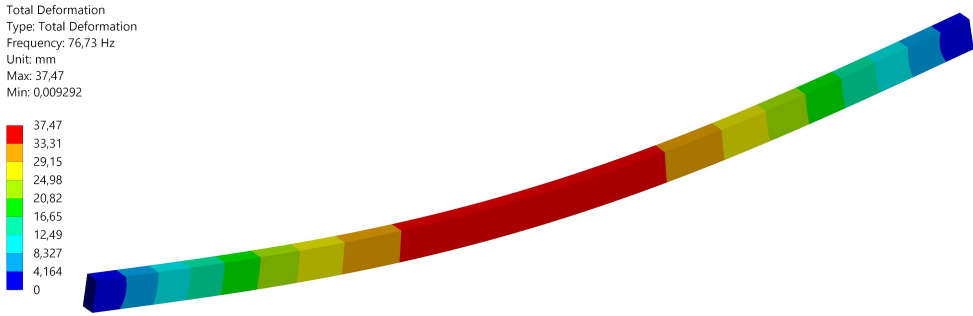


FIG. 8. Modal analysis result for the S-1 beam structure and the B-1 boundary condition.

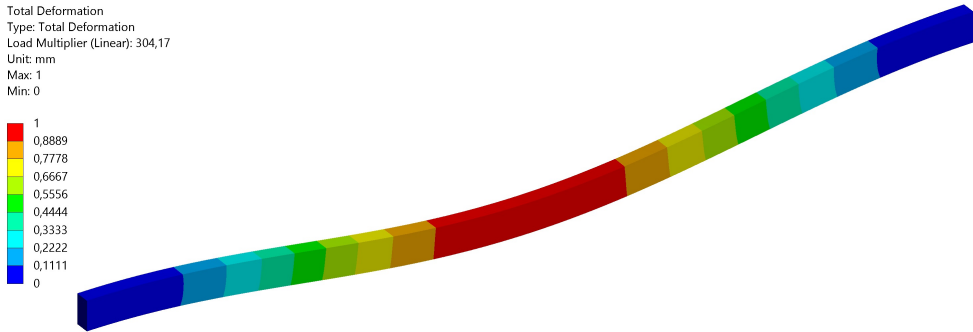


FIG. 9. Linear buckling analysis for the S-3 beam structure and the B-3 boundary condition.

TABLE 6. The results and comparison of the numerical FEM modal and buckling analyses for different structures and boundary conditions.

Beam	Structure	S-1	S-2	S-3
B-1	$10^3 \bar{F}_{o,CR} [-]$	0.6984	0.7201	0.7274
B-2		1.3734	1.4139	1.4273
B-3		2.5477	2.6173	2.6404
B-1	f_z [Hz]	76.73	77.91	78.30
B-2		116.52	118.17	118.72
B-3		163.41	165.52	166.21
B-1	$\Delta 10^3 \bar{F}_{o,CR} [\%]$	0.06	0.05	0.04
B-2		0.38	0.35	0.34
B-3		0.72	0.88	0.94
B-1	$\Delta f_z [\%]$	0.02	0.02	0.02
B-2		2.40	2.43	2.43
B-3		3.04	3.03	3.02

value, the results are incoherent with the values provided in Table 4. This is because the analytical solution considered the critical load in dimensionless form. To resolve the coherent value, it is necessary to transform Eq. (3.17) for the dimensionless critical force.

The results of the finite element analysis are provided in Table 6 for natural frequencies and buckling, considering all boundary conditions and different beam structures. These are compared with the outcome of the analytical study in the form of relative differences $\Delta 10^3 \bar{F}_{o,CR}^{(B-1)}$ and Δf_z . To verify the accuracy of the proposed model for shorter beams, additional numerical analyses are carried out, whose results are shown and compared to the previous study in Table 7.

TABLE 7. The results and comparison of the numerical FEM modal and buckling analyses.

λ [-]	15	20	25
$10^3 \bar{F}_{o,CR}^{(B-1)}$ [-]	2.55347	1.51041	0.991319
$f_z^{(B-1)}$ [Hz]	292.821	169.122	109.672
$\Delta 10^3 \bar{F}_{o,CR}^{(B-1)}$ [%]	0.94	0.30	0.05
$\Delta f_z^{(B-1)}$ [%]	0.31	0.12	0.05

6. Conclusions

The proposed form of Young's modulus distribution allows the study of structures with highly varied mechanical properties. Depending on the selected parameters, single- and three-layer beams can be analysed, with an optional stiffness ratio between the layers due to the generalised form of the proposed model.

As expected, the symmetrical properties of the structures studied resulted in the highest critical loads and natural frequencies among all the support conditions considered. Increasing the difference between the thicknesses of the faces leads to increased deterioration of results compared to the symmetrical structure with an equivalent core thickness. One must consider that the introduction of asymmetry does not significantly affect the mechanical behaviour of the analysed beams. For example, compared to a symmetrical structure, if one face is twice as thick as the other, the critical load is approximately 4% lower, while the decrease in natural frequency is merely 2%. These values are related to the simply supported boundary condition, which yields the highest discrepancy between symmetric and asymmetric structures.

To validate the consistency of the proposed analytical model, a numerical FEM study was undertaken for the coherent case studies. A comparison of

the results suggests that the maximum relative differences in natural frequency and critical load are 0.04% and 0.94%, respectively. One may notice that the relative differences are negligible for simply supported beams (B-1), whereas the introduction of fixed rotation supports (B-2, B-3) results in elevated but still limited discrepancies. It can be noted that the specific beam structure, i.e., Young's modulus distribution in the core, has a moderate impact on the results' consistency and can be considered somewhat ambiguous. Additional analyses revealed that a decrease in relative length leads to marginally increased relative differences between the numerical and analytical models. This shows that the proposed approach successfully compensates for shear effects.

Unlike numerous theories that study the buckling and vibrations of composites, the proposed approach allows for consideration of shear effects and achieves closed-form solutions. Taking into account the accuracy proven by the numerical FEM study, this approach can be considered original and suitable for solving vibration and buckling problems in functionally graded sandwich beam structures.

Acknowledgements

The paper was developed based on the scientific activities of the Łukasiewicz Research Network – Poznan Institute of Technology, Rail Vehicles Center, and the statutory activity of the Institute of Mathematics and the Institute of Applied Mechanics at Poznan University of Technology, funded by the Ministry of Science and Higher Education in Poland [grant number 0612/SBAD/3628 and 0213/SBAD/0117].

References

1. A. MAHI, E.A. ADDA BEDIA, A. TOUNSI, *A new hyperbolic shear deformation theory for bending and free vibration analysis of isotropic, functionally graded, sandwich and laminated composite plates*, Applied Mathematical Modelling, **39**, 9, 2489–2508, 2015.
2. T.-K. NGUYEN, T.T.-P. NGUYEN, T.P. VO, H.-T. THAI, *Vibration and buckling analysis of functionally graded sandwich beams by a new higher-order shear deformation theory*, Composite Part B: Engineering, **76**, 273–285, 2015.
3. D. CHEN, J. YANG, S. KITIPORNCHAI, *Free and forced vibrations of shear deformable functionally graded porous beams*, International Journal of Mechanical Sciences, **108-109**, 14–22, 2016.
4. M. FILIPPI, E. CARRERA, *Bending and vibrations analyses of laminated beams by using a zig-zag-layer-wise theory*, Composite Part B: Engineering, **98**, 269–280, 2016.

5. B.R. GONCALVES, A. KARTTUNEN, J. ROMANOFF, J.N. REDDY, *Buckling and free vibration of shear-flexible sandwich beams using a couple-stress-based finite element*, Composite Structures, **165**, 233–241, 2017.
6. S. KITIPORNCHAI, D. CHEN, J. YANG, *Free vibration and elastic buckling of functionally graded porous beams reinforced by graphene platelets*, Material Design, **116**, 656–665, 2017.
7. E. MAGNUCKA-BLANDZI, Z. WALCZAK, P. JASION, L. WITTENBECK, *Buckling and vibrations of metal sandwich beams with trapezoidal corrugated cores – the lengthwise corrugated main core*, Thin-Walled Structures, **112**, 78–82, 2017.
8. M. MOHAMMADIMEHR, S. SHAHEDI, *High-order buckling and free vibration analysis of two types sandwich beam including AL or PVC-foam flexible core and CNTs reinforced nanocomposite face sheets using GDQM*, Composite Part B: Engineering, **108**, 91–107, 2017.
9. K.K. ŻUR, *Free vibration analysis of elastically supported functionally graded annular plates via quasi-Green's function method*, Composite Part B: Engineering, **144**, 37–55, 2018.
10. K.K. ŻUR, *Quasi-Green's function approach to free vibration analysis of elastically supported functionally graded circular plates*, Composite Structures, **183**, 600–610, 2018.
11. K. MAGNUCKI, D. WITKOWSKI, J. LEWINSKI, *Bending and free vibrations of porous beams with symmetrically varying mechanical properties – Shear effect*, Mechanics of Advanced Materials and Structures, **27**, 4, 325–332, 2020.
12. K. XIE, Y. WANG, X. FAN, T. FU, *Nonlinear free vibration analysis of functionally graded beams by using different shear deformation theories*, Applied Mathematical Modelling, **77**, 1860–1880, 2020.
13. Y.-L. LEI, K. GAO, X. WANG, J. YANG, *Dynamic behaviors of single- and multi-span functionally graded porous beams with flexible boundary constraints*, Applied Mathematical Modelling, **83**, 754–776, 2020.
14. C.I. LE, N.A.T. LE, D.K. NGUYEN, *Free vibration and buckling of bidirectional functionally graded sandwich beams using an enriched third-order shear deformation beam element*, Composite Structures, **261**, 113309, 2021.
15. E. MAGNUCKA-BLANDZI, K. MAGNUCKI, W. STAWECKI, *Bending and buckling of a circular plate with symmetrically varying mechanical properties*, Applied Mathematical Modelling, **89**, 2, 1198–1205, 2021.
16. T.Q. HUNG, T.M. TU, D.M. DUC, *Free vibration analysis of sandwich beam with porous FGM core in thermal environment using mesh-free approach*, Archive of Mechanical Engineering, **69**, 3, 471–496, 2022.
17. K. MAGNUCKI, E. MAGNUCKA-BLANDZI, L. WITTENBECK, *Three models of a sandwich beam: Bending, buckling, and free vibrations*, Engineering Transactions, **70**, 2, 97–122, 2022.
18. K. MAGNUCKI, E. MAGNUCKA-BLANDZI, L. WITTENBECK, *Bending of generalized circular sandwich plate under concentrated force with consideration of an improved shear deformation theory*, Archives of Mechanics, **74**, 4, 267–282, 2022.
19. B. WANG, D. ZHANG, Y. CHEN, X. GUO, L. LI, *A new sandwich beam model with layer-to-layer boundary modified displacements based on higher-order absolute nodal coordinate formulation*, Journal of Sound and Vibration, **559**, 117748, 2023.

-
20. D. GOLIWAŚ, J. KUSTOSZ, K. MAGNUCKI, *Critical force and equilibrium paths of sandwich beams*, [in:] *Statics, Dynamics and Stability of Structures*, L. Czechowski, Z. Kołakowski [eds.], Lodz University of Technology, Chapter 5, pp. 99–117, 2023.
 21. K. MAGNUCKI, E. MAGNUCKA-BLANDZI, *A refined shear deformation theory of an asymmetric sandwich beam with porous core: bending problem*, *Applied Mathematical Modelling*, **124**, 624–638, 2023.

Received January 27, 2024; revised version June 6, 2024.

Published online September 5, 2024.
